Mitigating Range Ambiguity in High PRF Radar using Inter-Pulse Binary Coding

NADAV LEVANON, Life Fellow, IEEE
Tel Aviv University

The paper proposes a way to increase the energy within a coherent processing interval (CPI) using more pulses instead of longer pulses. Long coded pulses result in masking targets at close range and poor Doppler tolerance. Increasing the number of pulses implies high pulse repetition frequency (PRF), which suffers from range ambiguity and target folding. These drawbacks of a high PRF can be mitigated by inter-pulse coding. The approach suggested here should be attractive for close and mid range applications of radar, ground penetrating radar, ultrasound imaging, and more.

Manuscript received July 10, 2007; revised November 8 and December 22, 2007; released for publication March 22, 2008.

IEEE Log No. T-AES/45/2/933014.

Refereeing of this contribution was handled by A. Lanterman.

Author's address: Dept. of Electrical Engineering–Systems, Tel Aviv University, PO Box 39040, Tel Aviv, 69978, Israel, E-mail: (nadav@eng.tau.ac.il).

0018-9251/09/$25.00 © 2009 IEEE

I. INTRODUCTION

The probability of detection in coherent radar depends on the signal energy contained in the coherent processing interval (CPI). The Doppler (velocity) resolution depends on the duration of the CPI, which encourages the use of a coherent train of pulses. The delay (range) resolution depends on the bandwidth of the signal, which prompts using narrow pulses or modulated long pulses.

Increasing the energy in a CPI of a given duration, without increasing the peak power and without degrading the delay resolution, can be accomplished by using longer pulses or more pulses. A good review of the tradeoffs was given by Long and Harriger [1].

Two of the problems associated with long modulated pulses are long blind range regions from eclipsing during transmission and reduced Doppler tolerance of the individual pulse. A matched filter designed for non-zero Doppler is usually created using inter-pulse compensation of the Doppler-induced phase-ramp, usually through fast Fourier transform (FFT). On the other hand, intra-pulse phase-ramp compensation is rarely implemented. Therefore, the longer the pulse is, the larger is the destructive phase difference accumulated during its duration by the uncompensated Doppler-induced phase-ramp.

The other way to raise the energy (increasing the number of pulses within a given CPI) implies a radar mode of medium or high pulse repetition frequency (PRF). These modes can suffer from range ambiguity because the delay of returns from distant targets can be longer than the pulse repetition interval (PRI). The common approach to resolve range ambiguity is to use several CPIs within a single dwell, where each CPI has a different PRF. Resolving the true range and Doppler is performed noncoherently, using an "H out of P" decision, where H is usually 2 or 3 PRFs, while P can be as large as 8 PRFs [2, 3]. A "2 out of 8" detection decision implies that in some cases only 2 out of the 8 CPIs contribute energy to the detection process. This is a rather inefficient use of the transmitted energy.

This paper suggests a possible alternative to mitigating the range ambiguity in high PRF. It is based on inter-pulse binary coding during a single CPI that may occupy the entire dwell. The coding is based on an Ipatov binary sequence [4, 5], which yields ideal, low loss, periodic cross-correlation with a slightly mismatched sequence of the same length. Several examples of Ipatov binary sequences are listed in Appendix B. Their importance stems from the fact that except for Barker 4 there are no known binary sequences that yield ideal periodic autocorrelation. To exploit the sidelobe-free periodic cross-correlation, the number N_s of consecutive transmitted sequences has to

Authorized licensed use limited to: TEL AVIV UNIVERSITY. Downloaded on June 21, 2009 at 06:18 from IEEE Xplore. Restrictions apply.

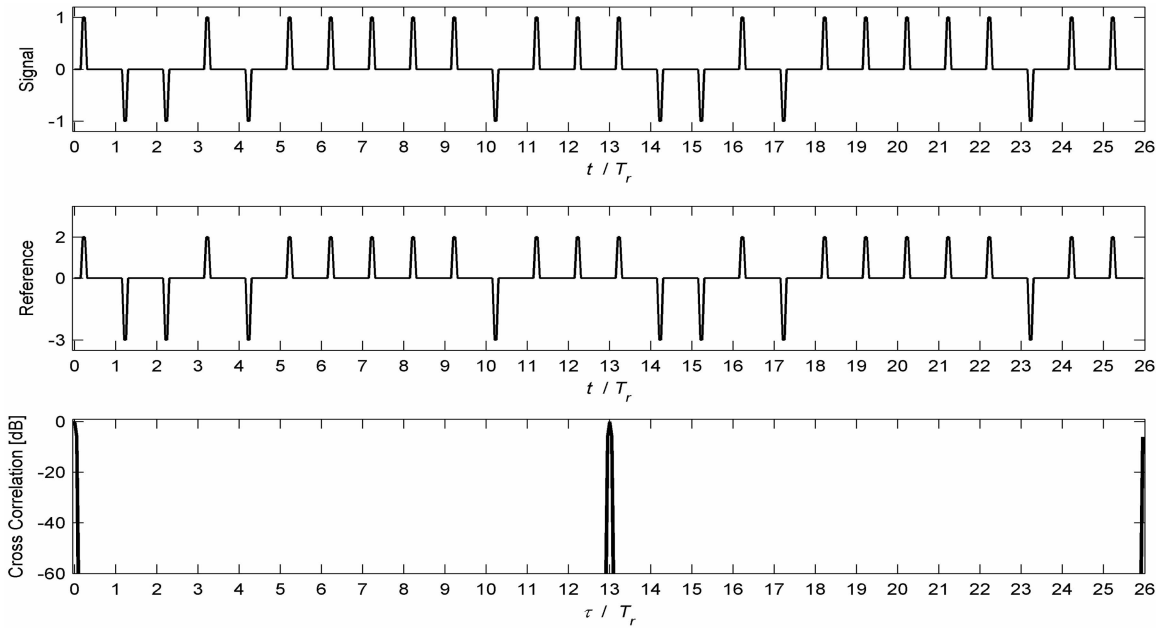

Fig. 1. Two periods out of high PRF pulse train with inter-pulse coding based on Ipatov 13 sequence. Signal (top), reference (middle), periodic cross-correlation (bottom).

TABLE I
Ipatov 13 Sequence

Sig	+1	−1	−1	+1	−1	+1	+1	+1	+1	+1	−1	+1	+1
Ref	+2	−3	−3	+2	−3	+2	+2	+2	+2	+2	−3	+2	+2

be larger than the number N_r of reference sequences stored in the receiver, by at least two, (e.g., $N_s = 18$ and $N_r = 16$).

The next section compares the delay (range) response of a high PRF system, inter-pulse coded by Ipatov 13 sequences, and a low PRF system with intra-pulse Barker 13 coding. The third section studies the delay-Doppler response of a coherent pulse train with inter-pulse Ipatov coding. Appendix A presents experimental results obtained in an indoor acoustic radar range. Appendix B lists several Ipatov binary sequences. Appendix C lists several Ipatov ternary sequences, which can also be used.

II. HIGH PRF WITH INTER-PULSE IPATOV PERIODIC CODING COMPARED WITH LOW PRF WITH INTRA-PULSE BARKER CODING

The suggested concept applies to low peak power radar (electromagnetic or acoustic) that has to cover both close and mid range. The low peak power restriction implies that the radar receiver is not blanked nor is it saturated during direct reception of the transmission, and the receiver can always perform linear processing.

Presently there are two options (of equal energy and equal range resolution) and neither can satisfy simultaneously both close and mid range:

(a) transmit a coherent train of few long coded pulses at large PRI and perform pulse compression,

(b) transmit a coherent train of many short pulses at short PRI.

In option (a), the pulse compression sidelobes of the direct signal can still hide close targets, dictating an unacceptable minimum range. In option (b), the direct signal and strong near clutter can hide distant targets because of range ambiguity.

The approach suggested in the present paper, labeled as (c), avoids both pitfalls. The radar will transmit many short pulses at short PRI, allowing unmasked detection at close range, and the inter-pulse coding will mitigate the range ambiguity and allow unmasked detection of targets at more distant ranges. To compare the different approaches, approach (c) will employ inter-pulse coding based on an Ipatov 13 code. The code and its mismatched reference are listed in Table I.

The actual transmitted signal is phase-coded. What is referred to as signal from now on will be its complex envelope. Thus, +1 and −1 refer to phases of 0 and π, respectively. The receiver performs synchronous detection, which yields digitized complex samples (one for each pulse, or coded element). The reference is a set of digital numbers stored in the receiver, with which the digitized detected samples are numerically correlated.

Two periods of a pulse-train signal following Table I appear in the top subplot of Fig. 1. The PRI is T_r, and the pulsewidth is $t_p = dT_r$, where d is the duty cycle. A relatively large d (= 0.1) was

Authorized licensed use limited to: TEL AVIV UNIVERSITY. Downloaded on June 21, 2009 at 06:18 from IEEE Xplore. Restrictions apply.

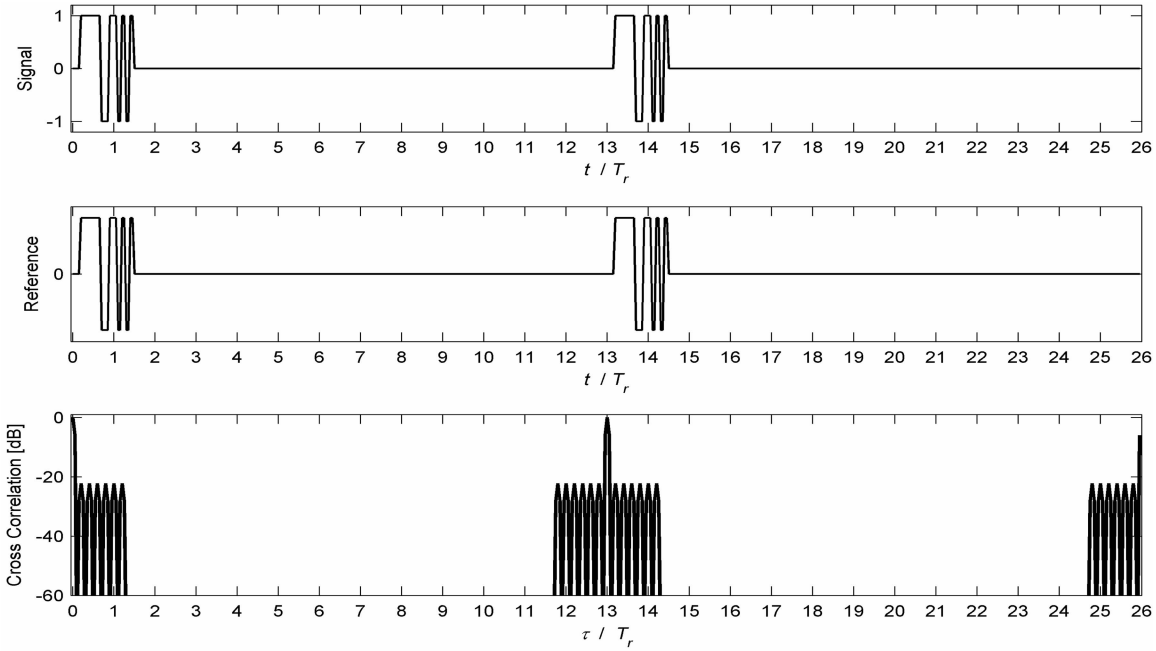

Fig. 2. Two periods out of low PRF pulse train with intrapulse coding based on Barker 13 sequence. Signal (top), matched reference (middle), periodic cross-correlation (bottom).

TABLE II
Details of Three Signal Options

	Pulse Coding						Delay Ambiguity		CPI =	Energy =
Option	Intra	Inter	t_b	t_p/t_b	PRI/t_b	M	MT_r	N_r	MN_rPRI	MN_rt_p
(a)	Barker 13	—	1	13	130	1	130	8	1040	104
(b)	—	—	1	1	10	1	10	104	1040	104
(c)	—	Ipatov 13	1	1	10	13	130	8	1040	104

chosen for figure clarity. The corresponding reference signal appears in the middle subplot. The resulting normalized periodic cross-correlation appears in the bottom subplot. It is labeled "ideal" because there are no sidelobes. The signal-to-noise ratio (SNR) loss caused by the mismatch is only 0.17 dB.

Fig. 1 demonstrates that despite the fact that the PRI is T_r, the delay ambiguity is MT_r, where $M = 13$ is the number of elements in the (Ipatov) sequence. For example, a target return at a delay $\tau_1 = 0.5T_r$ will appear at delays of $\tau = 0.5T_r, 13.5T_r, \ldots$, while a target return at a delay $\tau_2 = 10.5T_r$ will appear at delays of $\tau = 10.5T_r, 23.5T_r, \ldots$. Note, however, that if there is not enough isolation between the transmitter and the receiver, eclipsing will occur at intervals of T_r, not MT_r.

For comparison, a low PRF pulse train will be used, with intra-pulse Barker 13 coding, shown in Fig. 2. The two signals have identical energy, peak power, and CPI duration.

The complete set of signals in the comparison is as follows. In option (a), the receiver will process eight Barker 13 pulses with bit duration t_b and pulsewidth $t_p = 13t_b$. In option (b), the receiver will process 104 plain pulses of width $t_p = t_b$. In option (c), the receiver will process 8 sequences, each containing 13 plain pulses. The pulsewidth will be $t_p = t_b$. Ipatov 13 inter-pulse coding will be applied to each sequence. The CPI duration and the total energy will be the same in all three options. The signals' details are summarized in Table II. Note that the PRI in option (a) is different (much longer) than the PRI in options (b) and (c).

The minimum useable delay (range) is considered equal to the pulsewidth t_p. In option (a), there is a dependence on target reflection intensity. Using a matched filter, the sidelobe level for $t_b < \tau \leq t_p$ is -22.3 dB. A target within that delay span will be obscured, if its reflection is weaker by more than 22.3 dB relative to the direct signal. Note also that it is possible to use a mismatched filter, usually longer than the code, that will yield considerably lower sidelobes, but the sidelobe span will extend accordingly.

Table II shows that the new option (c) yields the lower minimum range and the higher unambiguous

Authorized licensed use limited to: TEL AVIV UNIVERSITY. Downloaded on June 21, 2009 at 06:18 from IEEE Xplore. Restrictions apply.

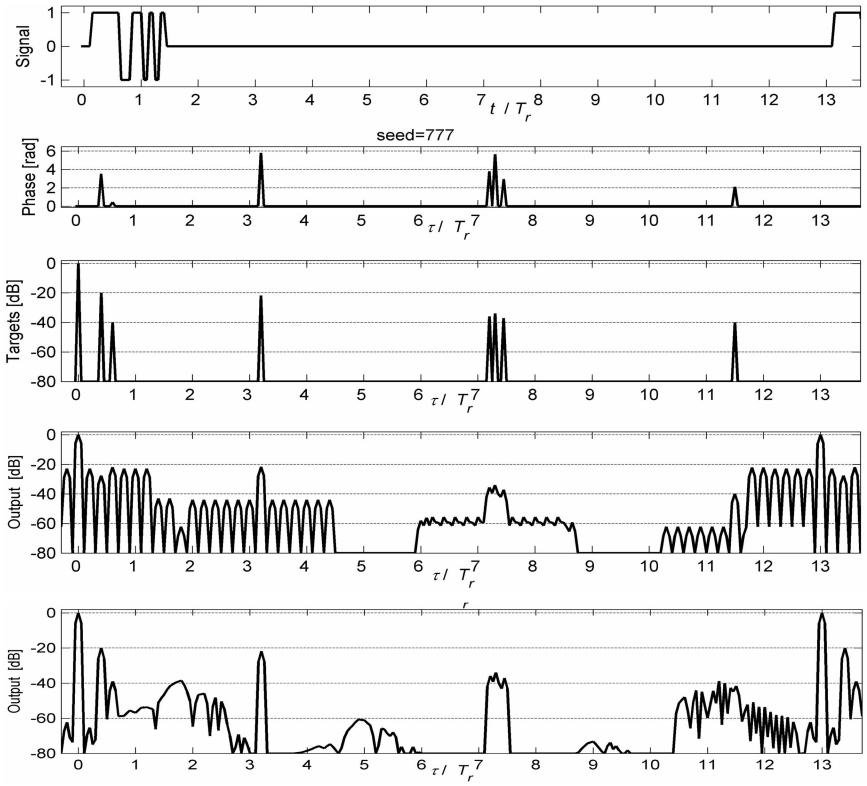

Fig. 3. Detecting target scene using signal option (a).

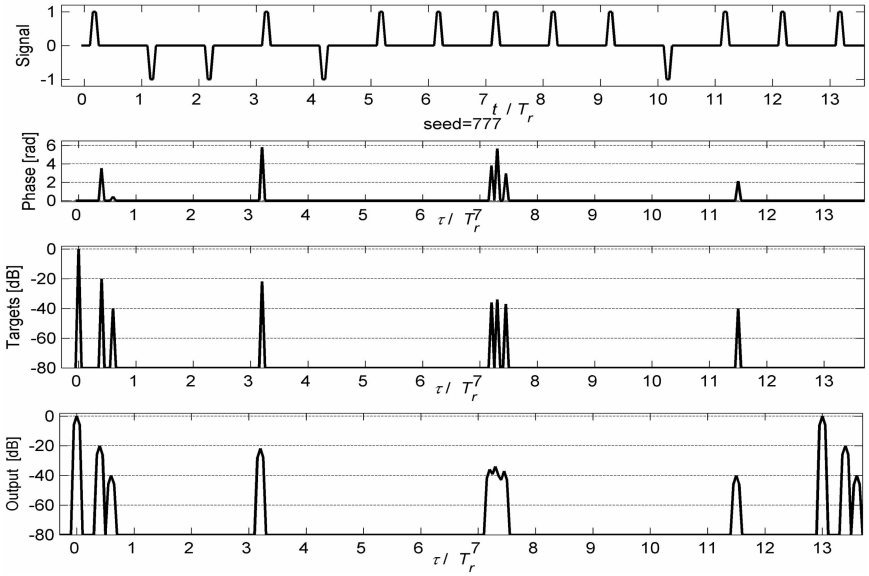

Fig. 4. Detecting target scene using signal option (c).

range. The penalty is the need to transmit at least two additional sequences, namely 25% more pulses (in this example), which means a 25% increase in dwell duration and transmitted energy.

The results achieved by the three signal options are demonstrated in Figs. 3–5, obtained from numerical simulations. The time axis in all the subplots in the three figures are equal and extends over 13 basic repetition periods T_r, where $T_r = 10t_b$. Consider first Fig. 3, which applies to signal option (a). The top subplot shows one period (out of 8) of the transmitted Barker 13 signal. The pulse duration is $t_p = 13t_b = 1.3T_r$. The beginning of the next pulse is also seen starting at $t = 13T_r$. The targets are described in the second and third subplots. Targets were placed only within the delay span $0 \leq \tau \leq 13T_r$. The "target" at zero delay represents the reception of the transmitted signal, and is referred to as the "direct signal." Each target is described by its phase in radians (2nd subplot) and its magnitude in dB

Authorized licensed use limited to: TEL AVIV UNIVERSITY. Downloaded on June 21, 2009 at 06:18 from IEEE Xplore. Restrictions apply.

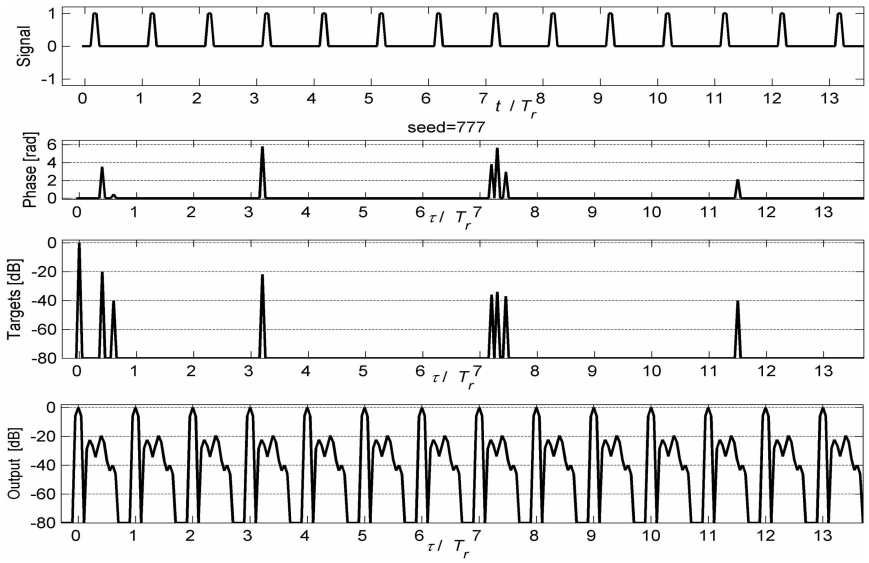

Fig. 5. Detecting target scene using signal option (b).

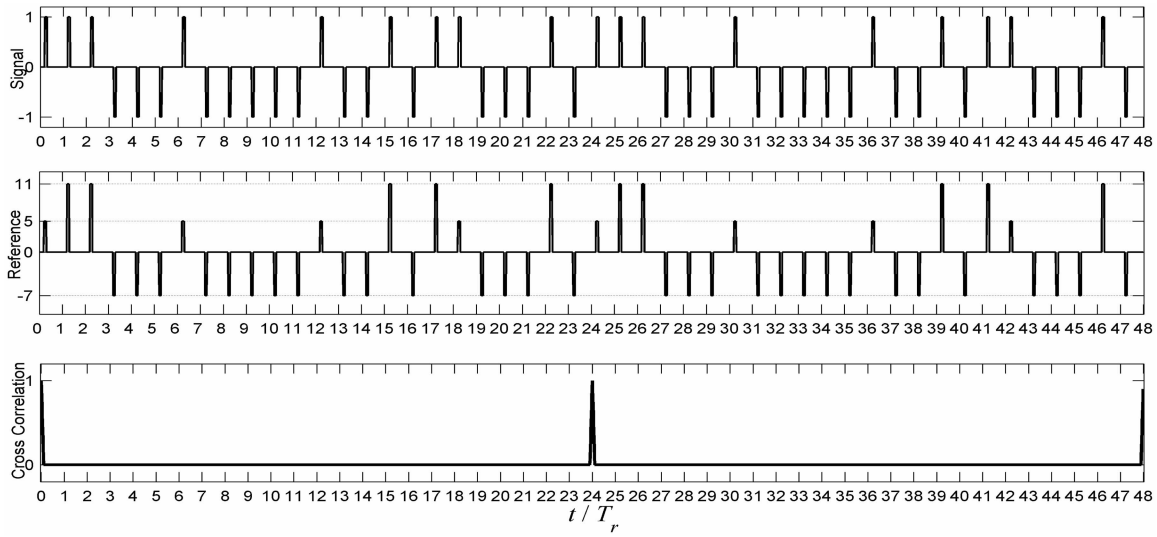

Fig. 6. Two periods of pulse train based on patov 24 sequence. Signal (top), reference (middle), periodic cross-correlation (bottom).

(3rd subplot). The 4th subplot displays the output (magnitude) of the matched filter. The last (bottom) subplot displays the output of a mismatched filter of length 39 designed for minimum integrated sidelobes. (See e.g., [5, sect. 6.6.].) Comparing the two lower subplots with the targets subplot, note that in the matched-filter case the sidelobes of the direct signal mask the first two targets. The last target is also barely distinguishable from the sidelobes of the folded direct signal (centered at $\tau = 13T_r$). Using a mismatched filter reduced the masking effect, but created sidelobes that may erroneously be assumed to be targets. In general, the presence of sidelobes is quite dominant, and if more weak targets were present, many would have been obscured by sidelobes. It should be pointed out that this was a noise-free simulation and the targets were stationary.

When the same target scene is illuminated by the new signal, option (c), dramatically better performance is observed (Fig. 4). The output replicates the targets very well. Of course, the targets' picture repeats itself after $\tau = 13T_r$, as expected in both options (a) and (c). The theoretical results depicted in Figs. 3 and 4 are supported by experimental results obtained in an indoor acoustic radar range (see Appendix A).

Theoretical results of using high PRF without inter-pulse coding (option (b)) are plotted in Fig. 5. The periodicity is now T_r rather than $13T_r$, which folds all the targets to within that short period, making resolution impossible.

III. DELAY-DOPPLER RESPONSE

A longer sequence (Ipatov 24) is used to study the delay-Doppler response when the receiver

Authorized licensed use limited to: TEL AVIV UNIVERSITY. Downloaded on June 21, 2009 at 06:18 from IEEE Xplore. Restrictions apply.

TABLE III
Ipatov 24 Sequence

Sig	+1	+1	+1	−1	−1	−1	+1	−1	−1	−1	−1	−1	+1	−1	−1	+1	−1	+1	+1	−1	−1	−1	+1	−1
Ref	+5	+11	+11	−7	−7	−7	+5	−7	−7	−7	−7	−7	+5	−7	−7	+11	−7	+11	+5	−7	−7	−7	+11	−7

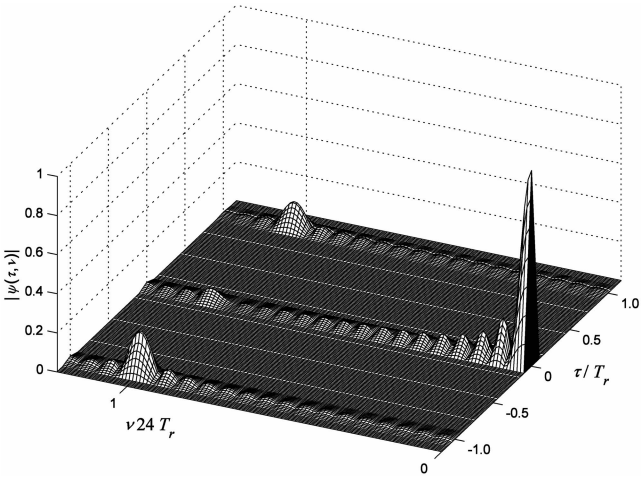

Fig. 7. Delay-Doppler periodic response of 16 periods of signal based on Ipatov 24 sequence. Zoom on $|\tau| < 1.1T_r$ and $0 \le \nu \le 1.2/MT_r$.

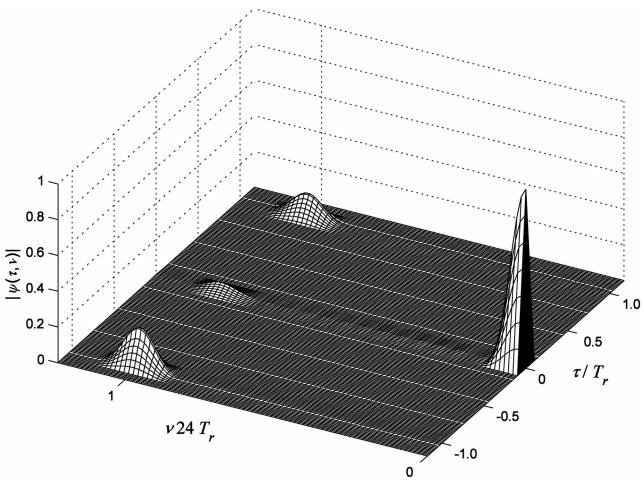

Fig. 9. Delay-Doppler periodic response of 16 periods of signal based on Ipatov 24 sequence, with Hamming-weighted reference. Zoom on $|\tau| < 1.1T_r$ and $0 \le \nu \le 1.2/MT_r$.

performs coherent cross-correlation with the nominal mismatched filter. The transmitted sequence is given in the top row of Table III, and its nominal reference is given in the bottom row. Note that with Ipatov 24, the reference is a three-valued sequence.

Two periods of a pulse-train signal following Table III appear in the top subplot of Fig. 6. The corresponding reference signal appears in the middle subplot. The resulting normalized periodic cross-correlation appears in the bottom subplot. The SNR loss caused by the mismatch is only 0.28 dB.

The main question regarding the delay-Doppler response of a cross-correlation receiver is how well the ideal periodic response holds with Doppler. We refrain from using the name "ambiguity function" because the reference is different from the conjugate of the signal. The calculations for the next figures of the delay-Doppler response use $N_s = 18$ periods of the transmitted signal and $N_r = 16$ periods of the reference (each period contains $M = 24$ pulses). Hence, the total number of pulses processed coherently is N_rM (= 384). The overall duration of the CPI is therefore N_rMT_r.

Fig. 7 displays the magnitude of the delay-Doppler periodic response $|\psi(\tau,\nu)|$ for the delay span of $|\tau| < 1.1T_r$ and Doppler span of $0 \le \nu \le 1.2/MT_r$. It is proper to refer to $\psi(\tau,\nu)$ as periodic because $N_r + 2 \le N_s$. The most important result is that the property of no recurrent lobes at $\tau = \pm T_r$, $\nu = 0$ extends to higher Doppler values. However, at $\tau = \pm T_r$, note the slow build-up of sidelobes with Doppler becoming small peaks at the inverse of the sequence period, namely at $\nu = 1/MT_r = 1/24T_r$. The mainlobe extends in delay over $|\tau| < t_p$, and in Doppler it reaches its first null at the inverse of the CPI duration, namely at $\nu = 1/N_rMT_r = 1/384T_r$ (not marked). The Doppler sidelobes follow a sinc function.

The Doppler sidelobes can be lowered by amplitude weighting the reference signal. The amplitudes of a Hamming-weighted reference pulse train (384 pulses) are shown in Fig. 8. Fig. 9 displays the delay-Doppler response when the unweighted signal is cross-correlated with the Hamming-weighted

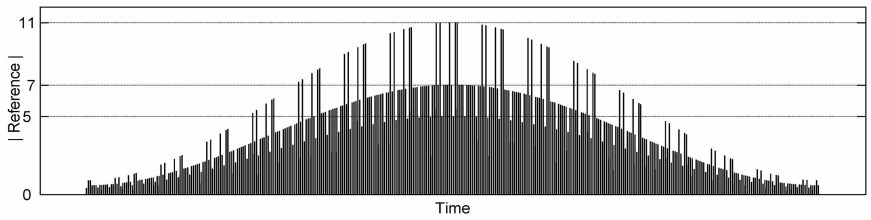

Fig. 8. Hamming-weighted amplitude of 16 periods of reference pulse train (based on Ipatov 24 sequence).

Authorized licensed use limited to: TEL AVIV UNIVERSITY. Downloaded on June 21, 2009 at 06:18 from IEEE Xplore. Restrictions apply.

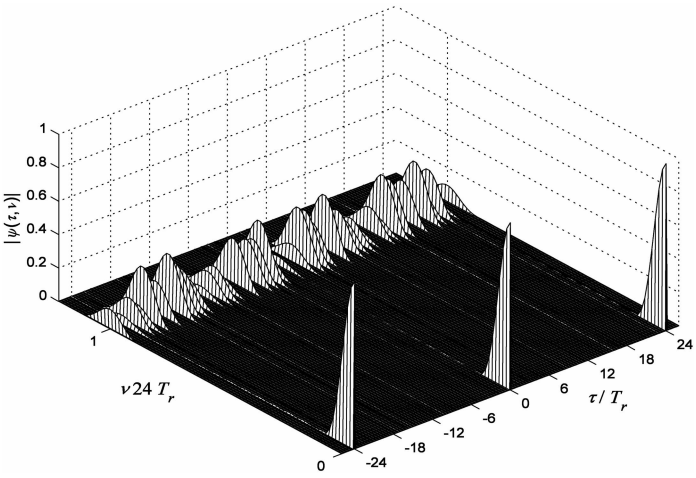

Fig. 10. Delay-Doppler periodic response of 16 periods of signal based on Ipatov 24 sequence, with Hamming-weighted reference. Zoom on $|\tau| < (M+1)T_r$ and $0 \le \nu \le 1.2/MT_r$.

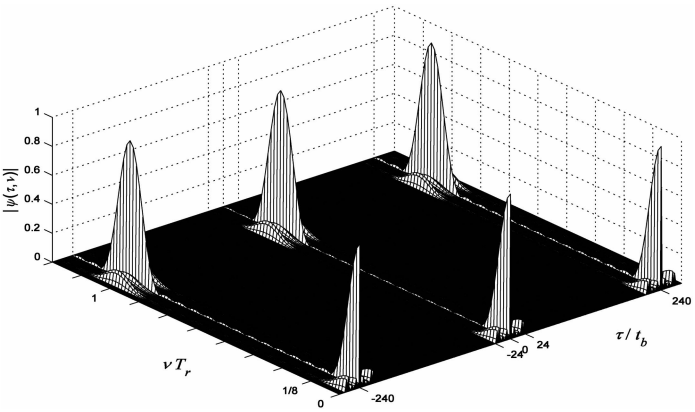

Fig. 11. Delay-Doppler periodic response of train of 16 pulses, intrapulse coded by MPSL 24, with Hamming-weighted reference. Zoom on, $|\tau| < 1.2T_r$ and $0 \le \nu \le 1.2/T_r$.

reference. Fig. 9 covers the same delay-Doppler span as Fig. 7. Comparing the two figures, Fig. 9 shows lower Doppler sidelobes but also an increase in the Doppler width of the mainlobe and of the recurrent Doppler lobes at $\nu = 1/MT_r = 1/24T_r$. Adding Hamming weight only in the receiver adds an SNR loss of about 1.5 dB.

A broader picture of the delay-Doppler response, when the reference is Hamming-weighted, is shown in Fig. 10. Here, the delay axis extends slightly beyond the recurrent delay lobes, at $\tau = \pm MT_r = \pm 24T_r$. Because the transmitted signal is longer than the reference signal by at least two periods, the first delay recurrent lobes (one on each side) are identical to the mainlobe. Without coding, there should have been recurrent delay lobes $\tau = \pm nT_r$, $n = 1,2,\ldots$. Fig. 10 demonstrates the absence of recurrent delay lobes (at zero Doppler) up to and including $n = M - 1 = 23$. Lower recurrent lobes of varying peaks do appear around $\nu = 1/MT_r = 1/24T_r$. Similar ridges will appear at $\nu = k/MT_r = k/24T_r$, $k = 2,3,\ldots$.

For comparison, Fig. 11 shows the delay-Doppler response of a coherent train of 16 identical pulses, intrapulse coded by a 24 element minimum peak sidelobe (MPSL) code (see [5, Table 6.3]), with Hamming weight on receive. The PRI is 24 times longer than the previous signal, to get the same range ambiguity and CPI duration. Fig. 11 exhibits the typical "bed of nails" response of a coherent pulse train, with recurrent mainlobes in both delay and Doppler, and with delay sidelobes extending on both sides of each mainlobe, for the pulse duration ($\pm 24t_b$). A bed of nails response can be obtained also from inter-pulse coding by using a polyphase sequence with ideal period autocorrelation (e.g., P3).

Inter-pulse binary coding does not rule out adding intrapulse coding to improve delay resolution. When each pulse of the inter-pulse coded signal is also coded internally using a Barker 5 binary code (and the duty cycle was increased) the resulting delay-Doppler response becomes as shown in Fig. 12. Fig. 13 shows a small section of such a signal, the reference (before

Authorized licensed use limited to: TEL AVIV UNIVERSITY. Downloaded on June 21, 2009 at 06:18 from IEEE Xplore. Restrictions apply.

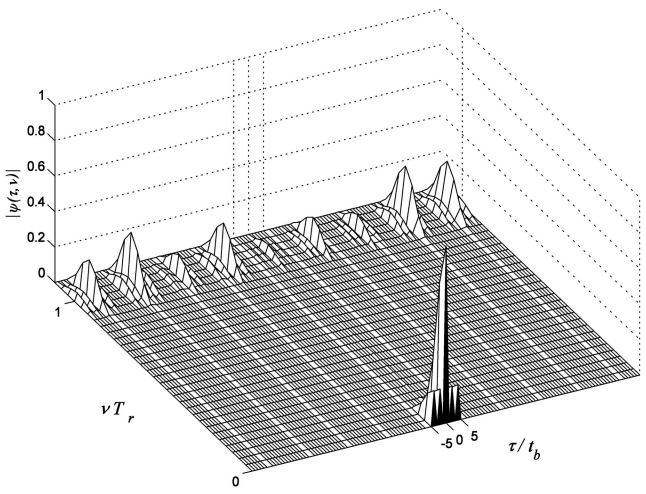

Fig. 12. Zoom on the delay-Doppler periodic response of 16 periods of signal based on Ipatov 24 sequence, including intrapulse Barker 5 coding, with Hamming-weighted reference.

adding Hamming weight), and the center of the cross-correlation (all using the same horizontal time scale).

Finally, note that the reference signal can be easily modified to create a response matched for a higher Doppler shift. Such a response is implemented by linearly stepping the phase of the consecutive pulses in the reference signal. Adding a phase step of $4\pi/(MN_r)$ between adjacent pulses creates the response seen in Fig. 14. This response exhibits a null at zero-Doppler. Without Hamming weighting, the smallest phase step for a null at zero Doppler would have been $2\pi/(MN_r)$.

IV. USING TERNARY SEQUENCES

Ternary sequences $\{1, 0, -1\}$ are avoided by conventional intrapulse compression, because a complex envelope whose value is "0" implies a break in the transmission. Our inter-pulse coding already has many breaks, as each code element is implemented in a separate pulse. In a ternary sequence a "0" element will simply imply skipping a pulse, so there is no reason to avoid ternary sequences if they exhibit ideal periodic correlation. It turns out that Ipatov has also described ternary sequences [6, 7] that exhibit ideal periodic autocorrelation. Their advantage is no SNR loss, because the signal and the reference are identical. Their disadvantage is lower energy per sequence duration, because some of the pulses are not transmitted. Examples of Ipatov's ternary sequences are given in Appendix C.

V. CONCLUSIONS

This paper showed how to transfer the task of pulse compression from a single long coded pulse to many short pulses with inter-pulse coding. Conventional pulse compression may not suit close-range applications, because in the output of the correlation processor the sidelobes of the direct signal may mask returns from close targets. The suggested inter-pulse coding is based on periodic Ipatov binary sequences, which exhibit ideal (sidelobe-free) cross-correlation with a slightly mismatched reference sequence. To maintain the periodic property, the number of transmitted sequences has to exceed the number of reference sequences by at least two. Using this kind of coding, the effective periodicity

Fig. 13. Small section out of pulse train using Ipatov 24 inter-pulse coding and Barker 5 intrapulse coding. Signal (top), reference before Hamming weighting (middle), correlation (bottom). Identical horizontal scale used in all subplots.

Authorized licensed use limited to: TEL AVIV UNIVERSITY. Downloaded on June 21, 2009 at 06:18 from IEEE Xplore. Restrictions apply.

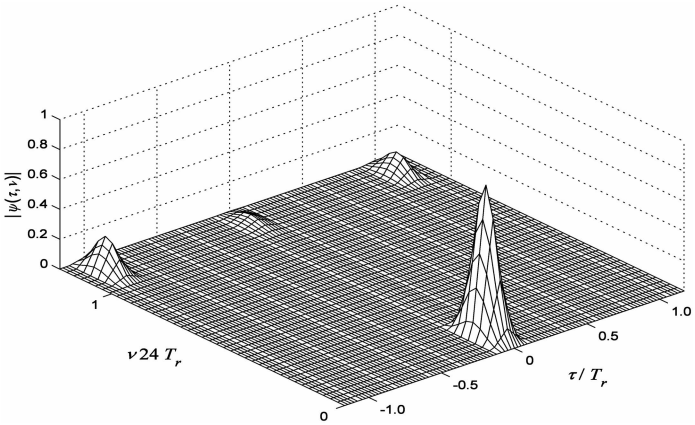

Fig. 14. Delay-Doppler periodic response of 16 periods of signal based on Ipatov 24 sequence, with Hamming-weighted and phase-ramped reference. Zoom on $|\tau| < 1.1T_r$ and $0 \le \nu \le 1.2/MT_r$.

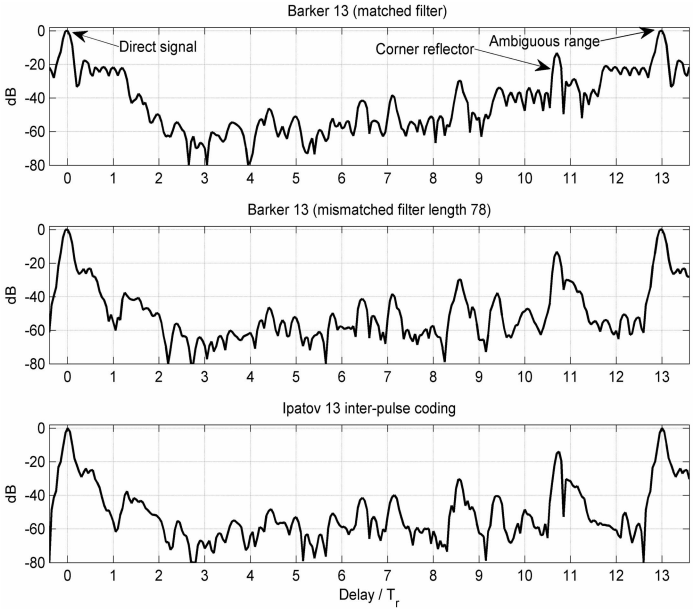

Fig. 15. Results from indoor acoustic radar.

increases from the actual pulse repetition period to the much longer sequence repetition period, thus mitigating range ambiguity and target folding. Since the correlation receiver needs to perform linear processing, the transmitter/receiver isolation must be large enough so that the direct signal will not cause saturation or blanking.

APPENDIX A. RESULTS FROM ACOUSTIC RADAR SIMULATOR

The signals described as options (a) and (c) were implemented in J. Mike Baden's indoor acoustic radar. The unambiguous range was 2.6 m. A corner reflector was placed about 0.4 m before the ambiguous range. The processed reflected scene is plotted in Fig. 15. The intrapulse coded Barker 13 signal (option (a)) was processed on receive by both a matched filter (length 13) and a mismatched filter (length 78). The corresponding outputs are shown in the top and middle subplots, respectively. The relatively high (-22 dB) sidelobes of the Barker 13 matched response are quite prominent in the top subplot, especially around the direct signal, the ambiguous range, and the corner reflector.

The inter-pulse coded Ipatov 13 signal was processed using its nominal mismatched filter given in Table I. Its processor output is shown in the bottom subplot of Fig. 15. In principle, this output should be sidelobe-free, and it is correct to deduce that the bottom subplot contains only genuine clutter returns. (The noise level is well below -80 dB.) The middle subplot can serve as an impartial judge. The middle subplot was obtained from the Barker 13 signal using a 78 element mismatched filter designed for minimum integrated sidelobes (ISL). Its peak sidelobe (PSL) is -65 dB. Hence, the middle subplot can be assumed as almost sidelobe-free. Indeed, the middle subplot strongly resembles the bottom subplot, thus supporting the conclusion that the inter-pulse periodic Ipatov coding yields sidelobe-free response in practice as well as in theory.

Authorized licensed use limited to: TEL AVIV UNIVERSITY. Downloaded on June 21, 2009 at 06:18 from IEEE Xplore. Restrictions apply.

APPENDIX B. ADDITIONAL IPATOV BINARY SEQUENCES

Length 21 (SNR loss=1.0 dB)

Signal: pnnppnpppppppppnpnppp (p=1,n=-1)

Reference: abbaabaaaaaaaaababaaa (a=3,b=-8)

Length 40 (SNR loss=0.37 dB)

Signal: pnnnpnnppnpppppnnppnpnpppppnpnpppppppppnpppp (p=1,n=-1)

Reference: abbbabbaabaaaabbaabababaaaabababaaaaaaabaaaa (a=5,b=-9)

Length 56 (SNR loss=0.69 dB)

Signal: ppnnnnnnnnnnnnnppnnpnnnppnnnnpnnnnnppnnpnpnpnppnpnnnnnnpn (p=1,n=-1)

Reference: abccccccccccccbaccacccaaccccbcccccaaccacacbcaacacccccac (a=43,b=65,c=-23)

Length 63 (SNR loss=0.3 dB)

Signal: ppppnpnpppppppppnnpppnnpnpnpnpppppppnppnnnnnpppnpnnpnnpnnpppnppnn (p=1,n=-1)

Reference: abaacacaaabaaaaccaabccacacacbaaaaaacabccccaaacbccaccaccbaacaacc (a=17,b=32,c=-28)

Length 121 (SNR loss=0.46 dB)

Signal: pnnnnnpppppnpppnnppnnnpnppnnnpnnnnnnpnpnnnnnpnnpnnnnnnppnpnpnnnnnnnnnnpnnnnnnnnpppnn
ppnpnpnnnnnnnpnppnnnnpnpnnnnnnppnnnpnnpnnnpnn (p=1,n=-1)

Reference: abbbbbaaaabaaabbaabbbabaabbbabbbbbabababbbbabbabbbbbbaabababbbbbbbbbabbbbbbbaaabb
bababababbbbbabaabbbabababbbbaabbbabbabbabb (a=27,b=-14)

APPENDIX C. EXAMPLES OF IPATOV'S TERNARY SEQUENCES

$$u_7 = [0\ 0\ -1\ 1\ 1\ 0\ 1]$$

$$u_{13} = [1\ 1\ 0\ 0\ -1\ -1\ 1\ 1\ -1\ 1\ 0\ 1\ 0]$$

$$u_{31} = [0\ -1\ 1\ 1\ -1\ 1\ 1\ 1\ -1\ 1\ 0\ -1\ 1\ 1\ 1\ 1\ -1\ -1\ 0\ -1\ 1\ -1\ -1$$
$$-1\ 1\ 0\ 1\ 0\ 1\ 1\ 0]$$

$$u_{57} = [1\ 1\ 1\ 1\ -1\ -1\ -1\ 1\ 1\ 0\ 1\ 1\ 1\ -1\ -1\ -1\ 1\ 1\ -1\ 1\ -1\ 1$$
$$1\ 1\ 1\ 1\ -1\ 1\ 0\ -1\ 1\ -1\ 0\ -1\ -1\ -1\ 1\ -1\ -1\ 0\ 1\ -1\ 1\ 1$$
$$-1\ -1\ 1\ 1\ 0\ -1\ 1\ -1\ 1\ 0\ 0\ 1\ 0]$$

$$u_{73} = [-1\ 1\ -1\ 1\ -1\ 0\ 1\ 1\ 1\ 1\ -1\ -1\ 1\ 1\ -1\ -1\ -1\ 1\ -1\ -1\ -1\ 0\ 1$$
$$1\ -1\ 1\ 0\ 1\ 1\ 1\ 1\ -1\ -1\ -1\ 1\ 1\ -1\ 1\ -1\ -1\ -1\ -1\ 1\ 1\ -1\ 0\ 1$$
$$1\ -1\ 1\ -1\ -1\ -1\ 1\ 0\ 1\ 1\ -1\ 1\ 1\ -1\ 1\ 1\ -1\ 0\ 0\ 1\ 0\ 1\ 11\ 0\ 1\ 1]$$

$$u_{91} = [-1\ 1\ -1\ 1\ -1\ 1\ 1\ 1\ 1\ 1\ -1\ 1\ 1\ 1\ -1\ -1\ -1\ -1\ 0\ 1\ -1\ -1$$
$$1\ -1\ 1\ 1\ 0\ 1\ 1\ -1\ 1\ 1\ 1\ 1\ -1\ 0\ -1\ 1\ 1\ 1\ 1\ -1\ 1\ 1$$
$$-1\ -1\ -1\ 1\ -1\ -1\ 1\ -1\ -1\ 1\ 1\ -1\ -1\ -1\ 0\ 1\ -1\ 1\ 1\ 1\ -1\ -1$$
$$-1\ -1\ 0\ -1\ 1\ 0\ 1\ -1\ -1\ 1\ 1\ 1\ -1\ 1\ 1\ -1\ 0\ 0\ -1\ 1\ 1\ 0\ 1\ 0\ 1]$$

Authorized licensed use limited to: TEL AVIV UNIVERSITY. Downloaded on June 21, 2009 at 06:18 from IEEE Xplore. Restrictions apply.

$$u_{133} = [1\ 1\ 0\ -1\ 1\ -1\ -1\ -1\ 1\ 1\ 0\ -1\ -1\ -1\ 1\ 1\ -1\ 1\ 1\ 1\ -1\ 1\ 1$$
$$-1\ -1\ -1\ -1\ 1\ -1\ 1\ -1\ 0\ -1\ 1\ 1\ 1\ -1\ 1\ -1\ 0\ 1\ -1\ 1\ -1\ -1$$
$$-1\ 1\ -1\ 1\ -1\ -1\ -1\ -1\ 1\ -1\ 1\ 1\ -1\ 1\ -1\ -1\ 1\ 1\ 1\ 0\ 1\ -1$$
$$-1\ -1\ 1\ 1\ 1\ 1\ 1\ 0\ 1\ 1\ -1\ -1\ 1\ 1\ -1\ -1\ 1\ -1\ -1\ 0\ 1\ 1$$
$$-1\ -1\ 1\ -1\ 1\ -1\ -1\ -1\ 1\ 1\ 1\ 1\ -1\ 1\ 1\ -1\ 1\ -1\ -1\ 1\ 1\ -1$$
$$1\ 0\ 0\ 1\ -1\ -1\ -1\ 1\ 1\ 1\ 1\ 1\ 1\ 1\ 1\ -1\ 0\ 1\ 1\ 0\ 1\ 0\ 1]$$

$$u_{183} = [-1\ 1\ -1\ 1\ -1\ -1\ 1\ -1\ 1\ 1\ 1\ 1\ 1\ 0\ -1\ -1\ 1\ 1\ -1\ -1\ 1\ 1\ -1$$
$$1\ -1\ -1\ -1\ 0\ 1\ 0\ 1\ 1\ 1\ 0\ 1\ -1\ 0\ -1\ -1\ -1\ -1\ -1\ 1\ -1\ 1\ 1$$
$$-1\ -1\ 0\ 1\ 1\ 1\ 1\ -1\ 1\ -1\ -1\ -1\ -1\ 1\ 1\ 1\ -1\ 1\ -1\ 1\ -1\ -1\ 1$$
$$1\ -1\ 1\ 1\ -1\ 1\ 0\ -1\ 1\ 1\ 1\ 1\ -1\ 1\ -1\ 1\ 1\ 1\ 1\ -1\ 1\ 1\ -1$$
$$1\ 1\ 1\ 1\ 1\ 1\ 1\ -1\ 1\ -1\ -1\ 1\ 1\ -1\ -1\ -1\ 1\ 0\ 1\ -1\ -1\ -1\ -1$$
$$-1\ 1\ 1\ -1\ -1\ 1\ 1\ 1\ 1\ 1\ 1\ 1\ -1\ -1\ 1\ 1\ 0\ 1\ -1\ 1\ 1\ -1\ 1\ -1$$
$$1\ -1\ -1\ 0\ 0\ -1\ -1\ 1\ -1\ 1\ -1\ 1\ 1\ -1\ -1\ 1\ 1\ -1\ -1\ 1\ 1\ -1\ 0\ -1$$
$$-1\ -1\ 1\ 1\ -1\ -1\ 0\ -1\ 1\ 1\ -1\ 0\ -1\ -1\ 1\ 1\ 1\ -1\ 1\ 1\ 1\ -1]$$

ACKNOWLEDGMENTS

The author wishes to thank Tal Cohen and Elad Shkedi from Tel Aviv University and J. Mike Baden from Georgia Tech. Research Institute for independently verifying the performance of the suggested signal in two different indoor acoustic radars.

REFERENCES

[1] Long, W. H., and Harriger, K. A.
Medium PRF for the AN/APG-66 radar.
Proceedings of the IEEE, **73**, 2 (Feb. 1985), 301–311.

[2] Hovanessian, S. A.
An algorithm for calculation of range in multiple PRF radar.
IEEE Transactions on Aerospace and Electronic Systems, **AES-12**, 2 (Mar. 1976), 287–290.

[3] Wiley, D., Parry, S., Alabaster, C., and Hughes, E.
Performance comparison of PRF schedules for medium PRF radar.
IEEE Transactions on Aerospace and Electronic Systems, **42**, 2 (Apr. 2006), 601–611.

[4] Ipatov, V. P., and Fedorov, B. V.
Regular binary sequences with small losses in suppressing sidelobes.
Radioelectron. a. Commun. Syst. (Radioelektronica), **27**, 3 (1984), 29–33.

[5] Levanon, N., and Mozeson, E.
Radar Signals.
Hoboken, NJ: Wiley, 2004, Sec. 6.5.

[6] Ipatov, V. P.
Ternary sequences with ideal periodic autocorrelation.
Radio Engineering and Electronic Physics, **24**, 10 (1979), 75–79.

[7] Ipatov, V. P.
Spread Spectrum and CDMA.
Chichester, England: Wiley, 2005.

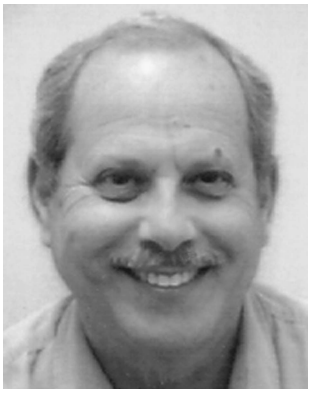

Nadav Levanon (S'67—M'70—SM'83—F'98—LF'06) is a professor at Tel Aviv University, Israel, where he has been a faculty member since 1970. He was Chairman of the EE-Systems Department during 1983–1985 and is presently the head of the Weinstein Research Institute for Signal Processing, and incumbent of the chair on Radar, Navigation and Electronic Systems. He spent sabbatical years at the University of Wisconsin, The Johns Hopkins University—Applied Physics Laboratory, and Qualcomm Inc, San Diego.

Dr. Levanon is a Life Fellow of the IEEE. His 1998 fellow citation is for "Contributions to radar signal analysis and detection." He is also a Fellow of the IET and member of the ION and AGU. He is the author of the book *Radar Principles* (Wiley, 1988) and coauthor of *Radar Signals* (Wiley, 2004).

Authorized licensed use limited to: TEL AVIV UNIVERSITY. Downloaded on June 21, 2009 at 06:18 from IEEE Xplore. Restrictions apply.